

## **Supporting Information for** Biological neurons act as generalization filters in reservoir computing

Takuma Sumi, Hideaki Yamamoto, Yuichi Katori, Koki Ito, Satoshi Moriya, Tomohiro Konno,  
Shigeo Sato, Ayumi Hirano-Iwata

Hideaki Yamamoto  
Email: [hideaki.yamamoto.e3@tohoku.ac.jp](mailto:hideaki.yamamoto.e3@tohoku.ac.jp)

### **This PDF file includes:**

Figures S1 to S7

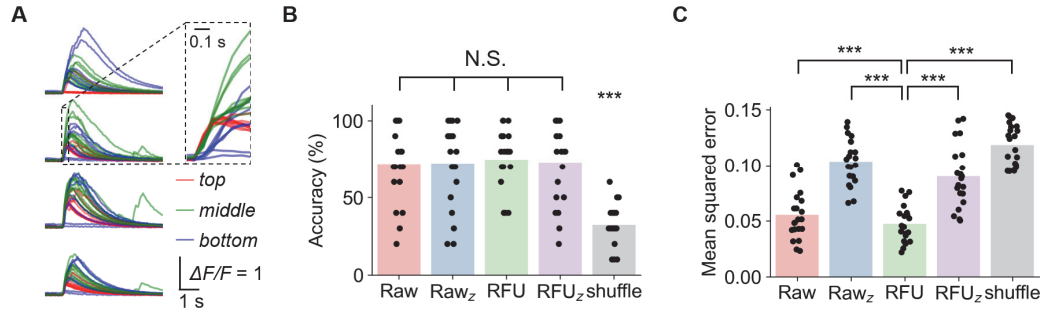


**Fig. S1.** (A) The dynamics of four representative neurons in an mBNN  $x(t)$  in response to the three rectangular input patterns (*top*: red, *middle*: green, *bottom*: blue). A close-up view of the response onset in the second neuron is shown in the inset, where characteristic rises depending on the input classes can be observed. (B) Classification accuracy and (C) MSE of the mBNN reservoir computed using different signals as  $x(t)$ : Raw, raw fluorescence intensity; Raw<sub>z</sub>, z-scored raw intensity; RFU, relative fluorescence unit; and RFU<sub>z</sub>, z-scored RFU. 'shuffle' denotes the values obtained using label-shuffled datasets with the RFU as  $x(t)$ . The accuracy calculated from the label-shuffled datasets are significantly lower than all other data. Filled circles represent a single mBNN, and bar heights show the mean. \*\*\* $p < 0.001$ ; N.S., no significance (two-sided paired  $t$ -test,  $n = 21$ ,  $df = 20$ ).

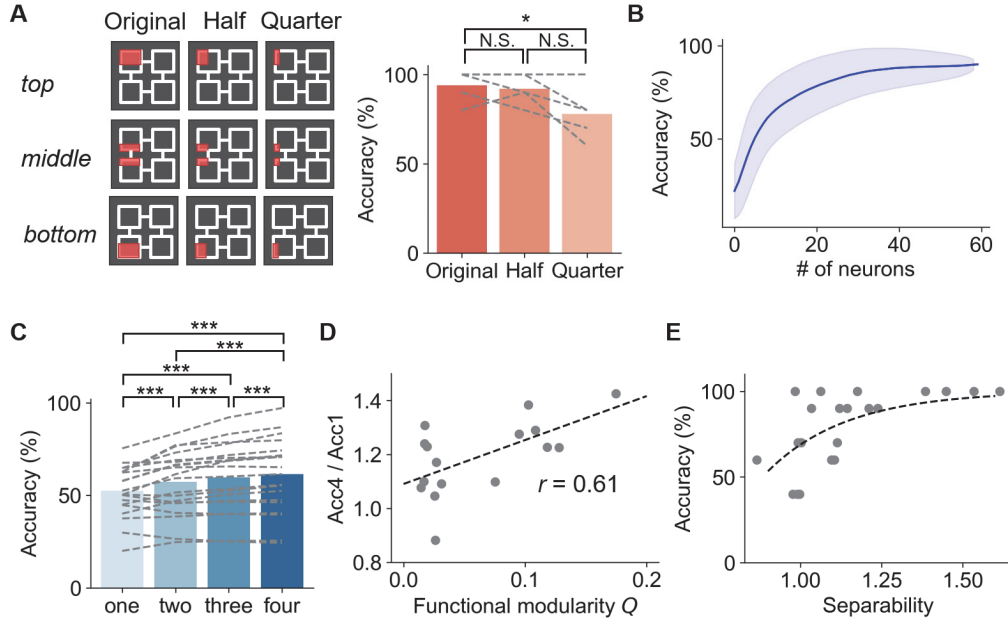


**Fig. S2.** Extended analysis of the reservoir computing performance in the spatial pattern classification task. (A) The effect of photostimulation area on the classification accuracy. Left panel, schematic representations of the original photostimulation area, as well as that reduced to be half and quarter in size. Right panel, the classification accuracy obtained using the original-size, half-size, and quarter-size stimulation. The accuracy significantly decreased when the photostimulation area was quartered.  $*p < 0.05$ ; N.S., no significance (two-sided paired  $t$ -test,  $n = 5$ ,  $df = 4$ ). (B) The influence of the number of neurons used for readout on the classification accuracy. The blue curve and the shaded error bar are the mean and the SD over different random selections ( $n = 10,000$ ) of neurons used for readout in a representative mBNN. Higher accuracy is obtained by increasing the number of reservoir neurons used for readout, although the precise number of neurons that saturate the accuracy varied from samples-to-samples. (C) The impact of spatial variability of reservoir neurons used in readout on the classification performance. The number of neurons used to calculate the readout was set to 15, and the neurons were randomly selected from one, two, three, or four modules.  $***p < 0.001$  (two-sided paired  $t$ -test,  $n = 21$ ,  $df = 20$ ). (D) The ratio of classification accuracy of mBNNs whose 15 neurons were selected from four modules (Acc4) to single module (Acc1) was positively correlated with the functional modularity of the network. The Pearson's correlation coefficient  $r = 0.61$  and  $p < 0.05$  (two-sided Pearson correlation test,  $n = 16$ ,  $df = 14$ ). (E) Classification accuracy as a function of separability. A single exponential curve fit is also shown to aid visualization (dashed line).

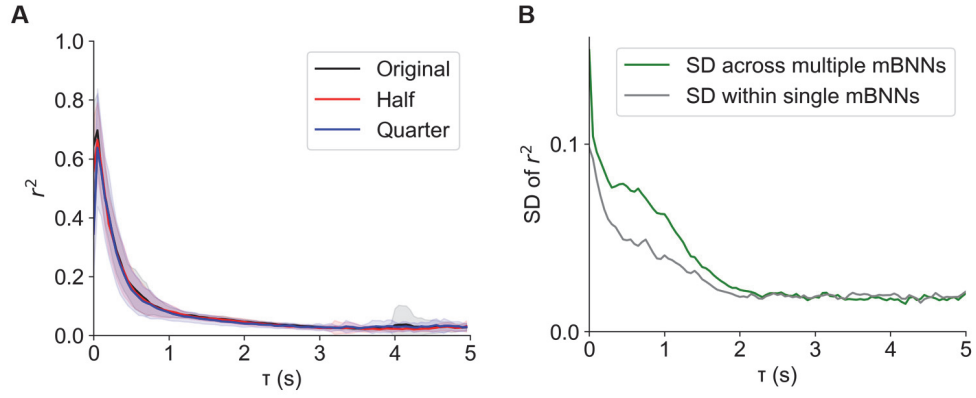


**Fig. S3.** (A) Effect of photostimulation area (see Fig. S2A) on the coefficient of determination ( $r^2$ ). The solid curves and the shaded error bars represent the means and the SDs, respectively, over mBNNs ( $n = 5$ ). The experimental conditions used to derive the curve for the 'original' photostimulation area is identical to that used in Fig. 3 and Fig. S3B, but the data come from different culture preparations. The forgetting curves remained mostly consistent irrespective of the reduction in the sizes of photostimulation with the mean residing within the standard deviations (shaded areas) of each curve. Thus, the forgetting curve presented in Fig. 3 represents the memory property that is characteristic the reservoirs and is independent of the input signal used to probe the property. (B) The SD of  $r^2$  across multiple mBNNs (green;  $n = 21$ ) and the mean of SDs within single mBNNs (gray;  $n = 21$ ), estimated using the 'original' photostimulation area. The variability across different mBNNs in stimulus responses was larger as compared to the variability within individual mBNNs.

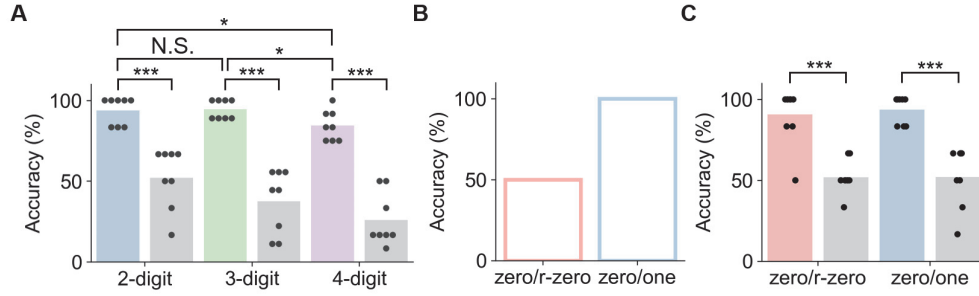


**Fig. S4.** (A) Classification accuracy of mBNN reservoirs in 2-digit ('zero' and 'one'), 3-digit ('zero', 'one', 'two'), and 4-digit ('zero', 'one', 'two', 'three') classification tasks. \* $p < 0.05$ ; \*\*\* $p < 0.001$ ; N.S., no significance (two-sided paired  $t$ -test,  $n = 8$ ,  $df = 7$ ). (B) The classification accuracy without mBNN. A linear decoder was trained to classify (i) a digit 'zero' and its temporally-reversed signal ('r-zero') (red) and (ii) digits 'zero' and 'one' (blue) directly from the photostimulation patterns. (C) Classification accuracy of mBNN reservoirs tasked to classify 'zero' and 'r-zero'. The accuracy in the zero-one classification task (as used in the main text) of the identical mBNNs are shown as a comparison. These data have been taken independently from those presented in the main figures. \*\*\* $p < 0.001$  (two-sided paired  $t$ -test,  $n = 9$ ,  $df = 8$ ). Filled circles represent single mBNNs, and bar heights show the mean. Gray bars show the values obtained using label-shuffled datasets.

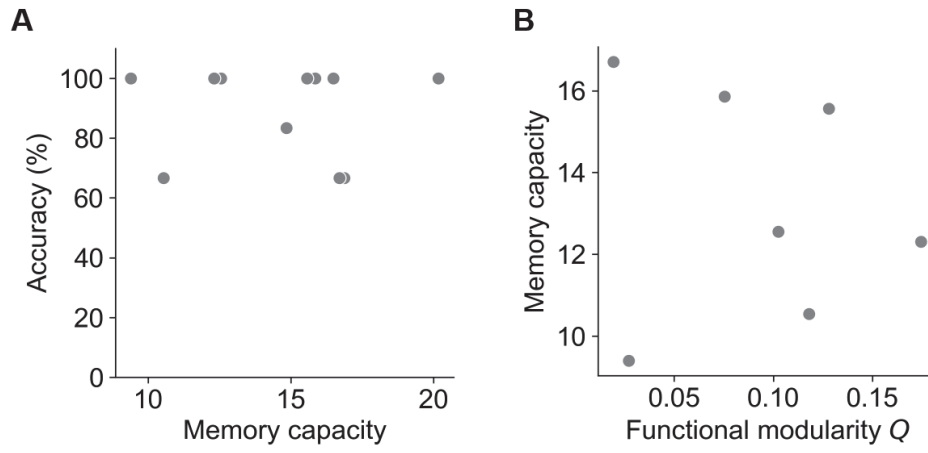


**Fig. S5.** (A) The classification accuracy of the spoken digit classification task does not correlate with the memory capacity of mBNNs. The Pearson's correlation coefficient  $r = -0.01$  and  $p = 0.97$  (two-sided Pearson correlation test,  $n = 11$ ,  $df = 9$ ). (B) The memory capacity does not correlate with the functional modularity of mBNNs. The Pearson's correlation coefficient  $r = -0.12$  and  $p = 0.79$  (two-sided Pearson correlation test,  $n = 7$ ,  $df = 5$ ).

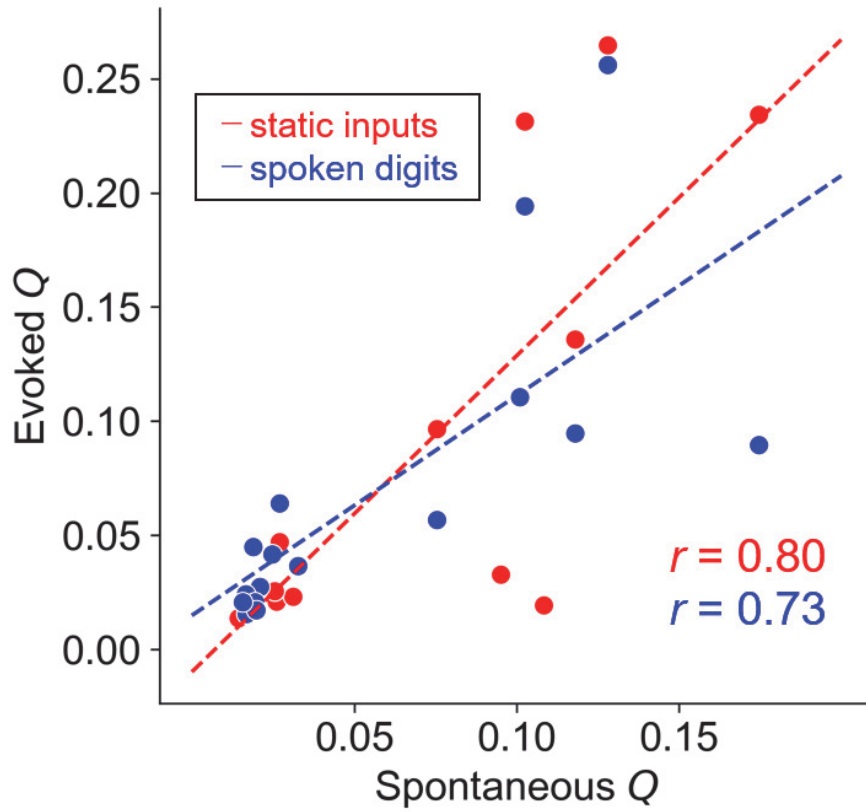


**Fig. S6.** Functional modularity  $Q$  calculated from the evoked activity strongly correlates with the value of  $Q$  calculated from the spontaneous activity recording in both the static pattern classification task (red) and the spoken digit classification task (blue). The Pearson's correlation coefficient  $r = 0.80$  ( $0.73$ ) for static inputs (spoken digits) and  $p < 0.001$  ( $0.01$ ) (two-sided Pearson correlation test,  $n = 16$ ,  $df = 14$ )

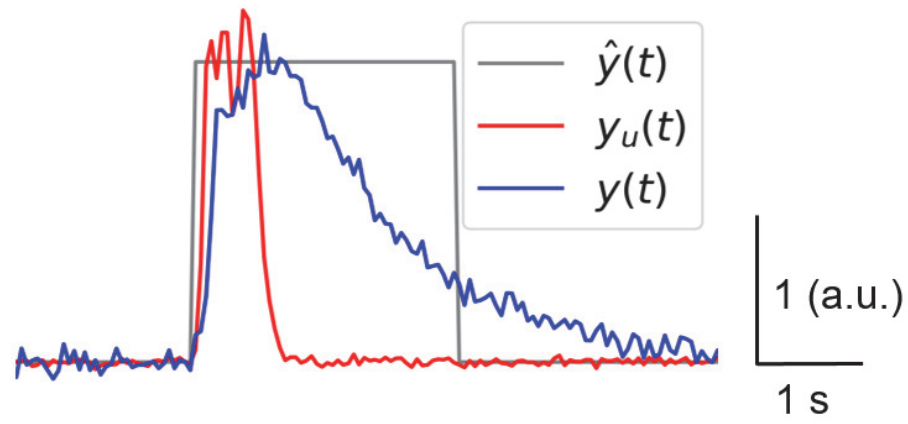


**Fig. S7.** Temporal relationship between the output signals generated by linear regression from the mBNN reservoir ( $y(t)$ , blue) with that generated from the input photostimulation pattern ( $y_u(t)$ , red). Gray curve is the target output ( $\hat{y}(t)$ ). Waveforms of an element corresponding to a correct estimate are shown during a spoken-digit classification task in response to an input of 'one'.